



# Sleek dual Extended Kalman Filter for Battery State of Charge and State of Health Estimation in Electric Vehicle Applications

Matteo Acquarone, Federico Miretti, and Daniela Misul Politecnico di Torino

Simona Onori Stanford University

**Citation:** Acquarone, M., Miretti, F., Misul, D., and Onori, S., "Sleek dual Extended Kalman Filter for Battery State of Charge and State of Health Estimation in Electric Vehicle Applications," SAE Technical Paper 2024-24-0023, 2024, doi:10.4271/2024-24-0023.

Received: 29 Apr 2024

Revised: 01 Jul 2024

Accepted: 08 Jul 2024

## Abstract

Accurate battery state estimation is crucial for the performance, safety, and durability of electric vehicle (EV) battery management systems (BMS). The model-based dual extended Kalman filter (DEKF) has been widely used for concurrent state of charge (SOC) and state of health (SOH) estimation. However, tuning the process and measurement covariance matrices of the DEKF is challenging and typically done through a trial and error process. In this work, a sleek version of the standard DEKF is formulated relying on a second-order equivalent circuit battery model (ECM) to estimate

the SOC and SOH of EV batteries. The proposed sleek DEKF estimates the capacity fading of the battery. The main advantage of the proposed formulation is the significant reduction in tuning effort. On the other hand, to account for the non-negligible resistance increase over battery lifespan, the ohmic resistance is here formulated as a function of the state of charge and available capacity. Finally, the effectiveness of the proposed method is demonstrated over laboratory data reproducing real-world driving scenarios. The results show that the proposed DEKF obtains high accuracy, comparable to the standard DEKF.

## Keywords

State of charge, State of health, State observer, Dual extended Kalman filter, Battery aging

## Introduction

State estimation is a crucial task for electric vehicle (EV) batteries. Two of the most important states to be estimated are the state of charge (SOC), linked with the remaining driving range, and the state of health (SOH), related battery degradation over its lifetime. Both SOC and SOH are non-measurable quantities whose value is crucial to inform the user, control the powertrain and thermal management systems, prevent damage and premature ageing of the battery pack. Furthermore, although they typically change over very different time scales, the two quantities are closely interrelated, as the state of charge is a function of the battery residual capacity [1].

Several joint SOC and SOH estimation algorithms have been developed under both data-driven and model-based approaches. Model-based methods have the advantage that they provide insights into battery

dynamics, e.g., equivalent circuit models (ECMs), and deliver accurate estimates across a wide range of conditions without the need for a high amount of training data. One of the most common model-based frameworks is the dual extended Kalman filter (DEKF), where one filter is used to estimate the SOC (as well as other relatively fast dynamics) and a second filter is used to estimate the slowly changing battery parameters (such as capacity and internal resistance) [2]. Many formulations of the DEKF have been proposed in the literature. These variants typically stem from: the equivalent circuit model that was used to derive the system dynamics; the characterization of the model parameters as constant values, SOC-dependent, or SOC-and temperature-dependent; the usage of a multiple timescale framework for the two filters.

One of the most commonly used frameworks is based on a second-order equivalent circuit model where

the open-circuit voltage (OCV) is SOC-dependent [3, 4, 5, 6, 7]. Still, different choices are possible in the design of the parameter estimator. For example, the authors of [3] define all the impedance parameters (three resistances and two capacitances) as parameters to be estimated, in addition to capacity, two hysteresis parameters, and two coefficients defining a linear equation for the OCV. In [4], all the impedance parameters are defined as parameters, though the time constants of the system are used instead of the capacitances. Oddly, the capacity was not defined as a parameter, but rather calculated using coulomb counting and the SOC estimates. A similar approach was followed by [6]. In [8], on the other hand, only the capacity and ohmic resistance are defined as parameters, whereas resistance-capacitance (RC) branches parameters are constants. The authors of [9] propose an advanced double extended Kalman filter algorithm that incorporates weighted multi-innovation and weighted maximum correlation entropy for the estimation of the capacity as the sole parameter. Following [10], in the remainder of this paper, we denote the standard DEKF as the variant that estimates both the capacity and the ohmic resistance  $R_0$ .

As described in [11], the DEKF for estimation of SOC and battery model parameters requires significant tuning effort. Although some works aim to provide useful suggestions for the tuning process [12], no standard guidelines for the tuning are available and the covariance matrices are typically tuned by trial and error. A sleek formulation of the dual extended Kalman filter is proposed in this work to reduce the number of tuning parameters that burdens the standard DEKF. While the standard DEKF estimates both the battery ohmic resistance and available capacity, the sleek DEKF (SDEKF) aims to estimate only one parameter, i.e., the available capacity. To account for the non-negligible resistance increase over aging, the ohmic resistance is approximated as a polynomial function of the SOC and available capacity. Thanks to the proposed formulation, a lower number of elements of the covariance matrices needs to be tuned for the SDEKF.

To prove the effectiveness of the SDEKF in EV real-world scenarios, the proposed estimation algorithm is tested on the aging dataset mimicking real-world driving profiles of EVs [13]. The SOC and SOH estimation results presented in this paper demonstrate that the sleek DEKF version achieves a comparable estimation accuracy to the standard DEKF, yet requiring lower number of parameters to be tuned.

## Battery Model

### SOC and SOH Definitions

The SOC is defined as the ratio between the remaining capacity stored in the battery and the actual available capacity  $Q_{cell}$  at a given time  $t$ , and is computed by

integrating the battery current through the following equation:

$$SOC(t) = SOC(t_0) + \frac{\int_{t_0}^t \eta(\tau) i(\tau) d\tau}{Q_{cell}(t)} \quad (1)$$

where  $t_0$  is the initial time instant,  $\eta$  is the Coulomb efficiency, set equal to 1 for Li-ion batteries [REF]. On the other hand, the SOH quantifies the battery degradation over its lifetime and is defined in this work as the ratio between  $Q_{cell}$  and the maximum available capacity of the fresh cell  $Q_{cell_0}$ :

$$SOH(t) = \frac{Q_{cell}(t)}{Q_{cell_0}} \quad (2)$$

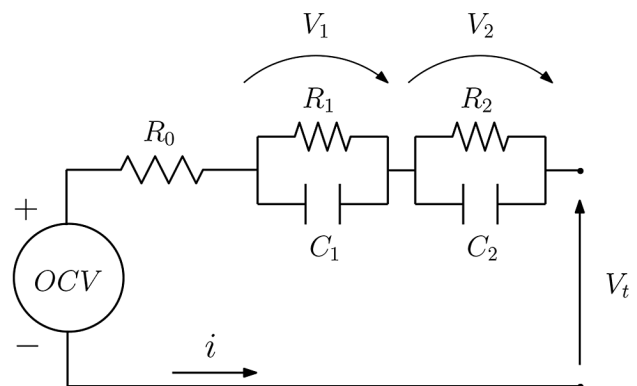
### Equivalent Circuit Model

To estimate SOC and SOH through a model-based method, a battery model must be adopted to describe the system dynamics. Among the different battery models used in the literature, we selected a second-order equivalent circuit model as a good compromise between model accuracy and computational complexity. The selected ECM, represented in Fig. 1, is characterized by several parameters, i.e., OCV, the ohmic resistance  $R_0$ , the resistances  $R_1$  and  $R_2$ , and capacitances  $C_1$  and  $C_2$  of the two RC branches.

All the ECM parameters are modeled as functions of the state of charge. On the other hand, not all the ECM parameters are equally affected by battery degradation. Indeed, the RC branch parameters vary less than the strongly varying capacity  $Q_{cell}$  and ohmic resistance  $R_0$ .

The second-order ECM is described as a nonlinear discrete-time state-space system. In the discrete-time state-space representation, with a sampling time  $T_s$ , the system dynamics (3) and the output equations (4) can be written as follows [14]:

**FIGURE 1** Second-order equivalent circuit model of the battery cell.



$$\begin{bmatrix} SOC_{k+1} \\ V_{1k+1} \\ V_{2k+1} \end{bmatrix} = \begin{bmatrix} 1 & 0 & 0 \\ 0 & e^{-\frac{T_s}{R_1 C_1}} & 0 \\ 0 & 0 & e^{-\frac{T_s}{R_2 C_2}} \end{bmatrix} \begin{bmatrix} SOC_k \\ V_{1k} \\ V_{2k} \end{bmatrix} + \begin{bmatrix} \frac{T_s}{Q_{cell}} \\ \left(1 - e^{-\frac{T_s}{R_1 C_1}}\right) R_1 \\ \left(1 - e^{-\frac{T_s}{R_2 C_2}}\right) R_2 \end{bmatrix} i_k, \quad (3)$$

$$V_{t_k} = OCV_k + V_{1k} + V_{2k} + R_0 i_k \quad (4)$$

where  $V_{1k}$  and  $V_{2k}$  are the voltages across the  $C_1$  and  $C_2$ , respectively,  $i_k$  is the current, and  $V_{t_k}$  is the terminal voltage. While the SOC dynamics are described by Coulomb counting, the dynamics of  $V_1$  and  $V_2$ , as well as the measurement equation for  $V_t$ , are computed using Kirchhoff's laws on the equivalent circuit.

## Sleek DEKF for SOC and SOH Estimation

### Fundamentals of Dual Extended Kalman Filter

The algorithm adopted in this work to estimate the SOC and SOH of the nonlinear battery system is based on extended Kalman filters, which approximate the nonlinearities of the systems's dynamics by linearizing the system model around the current state estimate [15].

In the DEKF, two separate filters are used to estimate the cell states  $x$  and parameters  $\theta$ . The state filter relies to the following equations (5) and (6) to update the state estimation:

$$x_{k+1} = f(x_k, u_k, \theta_k) + q_k^x \quad (5)$$

$$y_k = g(x_k, u_k, \theta_k) + r_k^x \quad (6)$$

where  $f(x_k, u_k)$  and  $g(x_k, u_k)$  are the nonlinear state transition function and nonlinear measurement function corresponding to ECM equations (3) and (4), respectively, while  $q_k^x$  and  $r_k^x$  are the process and measurement noise, respectively.

Under the main assumption that the parameters change slowly over time, the parameter filter equations can be written as follows:

$$\theta_{k+1} = \theta_k + d_k^\theta \quad (7)$$

$$d_k^\theta = g(x_k, u_k, \theta_k) + r_k^\theta \quad (8)$$

where  $q_k^\theta$  and  $r_k^\theta$  model a fictitious process noise to account for parameters' variations over cell life, and the measurement noise, respectively. The noises of the two filters are quantified by the process noise covariance matrices  $Q^x$  and  $Q^\theta$ , and measurement noise covariance matrix  $R^x$  and  $R^\theta$ . The other tuning matrices are the initial state  $P_0$  and parameter  $S_0$  covariance matrices which quantify the uncertainty of the initial estimate of the states and parameters respectively. The comprehensive workflow of the DEKF algorithm is depicted in Algorithm 1.

**ALGORITHM 1** Block diagram of system and sleek dual extended Kalman filter.

Initialize  $\hat{x}_0, P_0, Q^x, R^x$

Initialize  $\hat{\theta}_0, S_0, Q^\theta, R^\theta$

**Definition:**  $A_k = \frac{\partial f(x_k, u_k, \hat{\theta}_k^+)}{\partial x_k} \Big|_{x_k = \hat{x}_k^+}$ ,

$C_k^x = \frac{\partial g(x_{k+1}, u_{k+1}, \hat{\theta}_k^+)}{\partial x_k} \Big|_{x_{k+1} = \hat{x}_{k+1}^-}$

**Definition:**  $C_k^\theta = \frac{dg(\hat{x}_{k+1}^-, u_{k+1}, \theta)}{d\theta} \Big|_{\theta = \hat{\theta}_{k+1}^-}$

**for**  $k \leftarrow 1$  **to**  $n$  **do**

Parameters prediction step

$$\hat{\theta}_{k+1}^- = \hat{\theta}_k^+$$

$$S_{k+1}^- = S_k^+ + Q^\theta$$

State prediction step

$$\hat{x}_{k+1}^- = f(\hat{x}_k^+, u_k)$$

$$P_{k+1}^- = A_k P_k^+ A_k^T + Q^x$$

State update step

$$K_k^x = P_{k+1}^- (C_k^x)^T (C_k^x P_{k+1}^- (C_k^x)^T + R^x)^{-1}$$

$$\hat{x}_{k+1}^+ = \hat{x}_{k+1}^- + K_k^x (y_k - \hat{y}_k)$$

$$P_{k+1}^+ = (I - K_k^x C_k^x) P_{k+1}^-$$

Parameters update step

$$K_k^\theta = S_{k+1}^- (C_k^\theta)^T (C_k^\theta S_{k+1}^- (C_k^\theta)^T + R^\theta)^{-1}$$

$$\hat{\theta}_{k+1}^+ = \hat{\theta}_{k+1}^- + K_k^\theta (y_k - \hat{y}_k)$$

$$S_{k+1}^+ = (I - K_k^\theta C_k^\theta) S_{k+1}^-$$

**end for**

After the initialization of parameter and state estimates to their best guesses, the two separate filters estimate states and parameters at each time step, interchanging some information. Following the formulation of [11], the equation to obtain the Jacobian  $C_k^\theta$  can be written as:

$$C_k^\theta = \left. \frac{dg(\hat{x}_{k+1}^-, u_{k+1}, \theta)}{d\theta} \right|_{\theta = \hat{\theta}_{k+1}^-}$$

$$\frac{dg(\hat{x}_{k+1}^-, u_{k+1}, \theta)}{d\theta} = \frac{\partial g(\hat{x}_{k+1}^-, u_{k+1}, \theta)}{\partial \theta} + \frac{\partial g(\hat{x}_{k+1}^-, u_{k+1}, \theta)}{\partial \hat{x}_{k+1}^-} \frac{d\hat{x}_{k+1}^-}{d\theta} \quad (9)$$

$$\frac{d\hat{x}_{k+1}^-}{d\theta} = \frac{\partial f(\hat{x}_k^+, u_k, \theta)}{\partial \theta} + \frac{\partial f(\hat{x}_k^+, u_k, \theta)}{\partial x_k^+} \frac{dx_k^+}{d\theta}$$

$$\frac{dx_k^+}{d\theta} = \frac{dx_k^-}{d\theta} - K_k^x \frac{dg(\hat{x}_k^-, u_k, \theta)}{d\theta}$$

where the derivatives  $\frac{dx_k^-}{d\theta}$  and  $\frac{dg(\hat{x}_k^-, u_k, \theta)}{d\theta}$  are initialized to zero for  $k$  equal to zero.

The exchange of information between the system and DEKF is shown in the block diagram of Fig. 2. This schematic is valid for both standard DEKF and SDEKF.

## Standard DEKF for SOC and SOH Estimation

For both the standard DEKF and SDEKF for SOC and SOH estimation, the state vector  $x_k$ , the measured input  $u_k$ , and the measurement output  $y_k$  are the following:

$$x_k = [SOC_k, V_{1k}, V_{2k}] \quad (10)$$

$$u_k = i_k \quad (11)$$

$$y_k = V_{tk} \quad (12)$$

Between all the ECM parameters, only the strongly varying parameters over the cell life are typically estimated to reduce the computational complexity of the algorithm. Since  $Q_{cell}$  and  $R_0$  are usually identified as the most varying parameters over battery lifetime, we refer to the standard DEKF as the DEKF formulation that estimates the parameters:

$$\theta = [Q_{cell}, R_0] \quad (13)$$

For the standard DEKF, the computation of the derivatives of the  $C_k^\theta$  matrix is obtained through the following equations:

$$\frac{\partial g(\hat{x}_{k+1}^-, u_{k+1}, \theta)}{\partial \theta} = [0 \quad i_{k+1}] \quad (14)$$

$$\frac{\partial g(\hat{x}_{k+1}^-, u_{k+1}, \theta)}{\partial \hat{x}_{k+1}^-} = \left[ \left. \frac{\partial OCV}{\partial SOC} \right|_{\hat{x}_{k+1}^-} \quad 1 \quad 1 \right] \quad (15)$$

$$\frac{\partial f(\hat{x}_k^+, u_k, \theta)}{\partial \theta} = \begin{bmatrix} -\frac{T_s}{Q_{cell}^2} i_k & 0 \\ 0 & 0 \\ 0 & 0 \end{bmatrix} \quad (16)$$

$$\frac{\partial f(\hat{x}_k^+, u_k, \theta)}{\partial \hat{x}_k^+} = \begin{bmatrix} 1 & 0 & 0 \\ 0 & e^{-\frac{T_s}{R_0 C_1}} & 0 \\ 0 & 0 & e^{-\frac{T_s}{R_0 C_2}} \end{bmatrix} \quad (17)$$

The DEKF for estimation of SOC and parameters has the main disadvantage of requiring a significant tuning effort [11]. Moreover, this tuning is highly correlated to the sensitivity of the model parameters with respect to the battery data and significantly affects the filter performance.

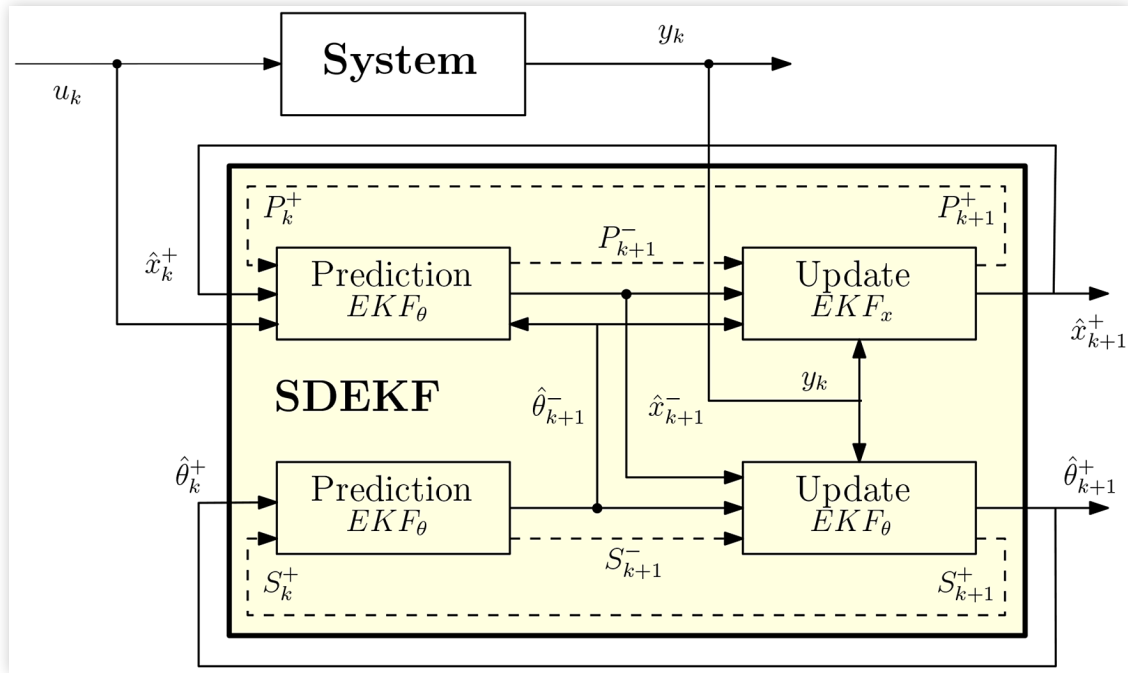
## Sleek DEKF for SOC and SOH Estimation

A sleek formulation of the DEKF for SOC and SOH estimation is proposed in this work to reduce the tuning effort. The key strategy for simplifying the estimation problem is to reduce the number of parameters that need to be estimated, consequently reducing the number of tuning elements of the covariance matrices of the DEKF. Hence, in the SDEKF just one parameter is estimated, i.e., the available capacity:

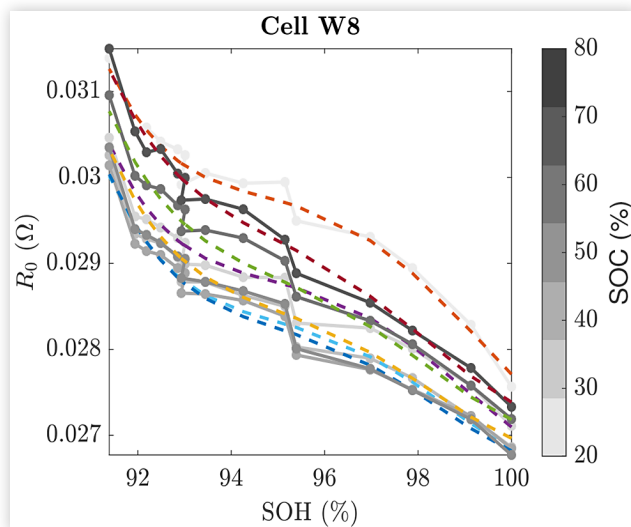
$$\theta = [Q_{cell}] \quad (18)$$

However, completely disregarding the ohmic resistance increase throughout the cell lifetime could lead to erroneous SOC and SOH estimation due to significant inaccuracies in the battery model. Battery internal resistance  $R_0$  is generally considered as a function of different quantities, such as the state of charge and the battery temperature. Moreover, in several previous works [16], a strong relationship between capacity fading and ohmic resistance increase has been noted. For instance, a strong linear correlation between the two aging quantities is highlighted in [17]. However,  $R_0$  cannot be formulated as a linear function of the capacity fading for all the aging datasets and battery chemistries with an acceptable level of accuracy. Therefore, to account for  $R_0$  variation and develop a formulation of the DEKF that is adaptable to a wider range of aging datasets, the ohmic resistance is modeled in the sleek DEKF as a polynomial function of the SOC and available capacity  $Q_{cell}$ :

$$R_0(SOC, Q_{cell}) = a_1 \cdot SOC^3 + a_2 \cdot SOC^2 \cdot Q_{cell} + a_3 \cdot SOC^2 + a_4 \cdot SOC \cdot Q_{cell}^2 + a_5 \cdot SOC \cdot Q_{cell} + a_6 \cdot SOC + a_7 \cdot Q_{cell}^3 + a_8 \cdot Q_{cell}^2 + a_9 \cdot Q_{cell} + a_{10} \quad (19)$$

**FIGURE 2** Block diagram of system and sleek dual extended Kalman filter.

where  $a_i$  is the  $i^{\text{th}}$  coefficient of the polynomial function. It is worth noting that the  $R_0$  dependence from temperature can be neglected in our work, due to the constant environment temperature of the aging dataset [13]. The polynomial degree is selected equal to 3 as a good compromise between approximation accuracy and polynomial complexity. In Fig. 3, the experimental  $R_0$  and its polynomial approximation over cell W8 data from the dataset [13] are depicted in greys and colors, respectively, as a function of SOC and SOH. The value of the ohmic resistance is computed for each SOH value from the

**FIGURE 3** Ohmic resistance  $R_0$  as a function of the SOC and SOH. While the grey lines are the real data points obtained through the HPPC tests, the colored lines represent its polynomial approximation as a function of SOC and capacity.

correspondent HPPC test [18]. As expected, a smooth increase in internal resistance is observed as the battery ages.

Thanks to the polynomial approximation of  $R_0$ , it is possible to analytically compute the partial derivatives  $\frac{\partial R_0}{\partial Q_{\text{cell}}}$  and  $\frac{\partial R_0}{\partial \text{SOC}}$  and the different terms of the matrix  $C_k^\theta$  of the SDEKF are computed as follows:

$$\frac{\partial g(\hat{x}_{k+1}^-, u_{k+1}, \theta)}{\partial \theta} = \begin{bmatrix} \frac{\partial R_0}{\partial Q_{\text{cell}}} i_k \end{bmatrix} \quad (20)$$

$$\frac{\partial g(\hat{x}_{k+1}^-, u_{k+1}, \theta)}{\partial \hat{x}_{k+1}^-} = \begin{bmatrix} \frac{\partial \text{OCV}}{\partial \text{SOC}} + \frac{\partial R_0}{\partial \text{SOC}} i_k & 1 & 1 \end{bmatrix} \quad (21)$$

$$\frac{\partial f(\hat{x}_k^+, u_k, \theta)}{\partial \theta} = \begin{bmatrix} -\frac{T_s}{Q_{\text{cell}}^2} i_k \\ 0 \\ 0 \end{bmatrix} \quad (22)$$

$$\frac{\partial f(\hat{x}_k^+, u_k, \theta)}{\partial \hat{x}_k^+} = \begin{bmatrix} 1 & 0 & 0 \\ 0 & e^{-\frac{T_s}{R_1 C_1}} & 0 \\ 0 & 0 & e^{-\frac{T_s}{R_2 C_2}} \end{bmatrix} \quad (23)$$

## Results

In this section, the estimation accuracy of the standard DEKF and sleek DEKF are assessed over the aging dataset from [13]. First, a comparison analysis is carried out to

highlight that the sleek DEKF can achieve comparable performance to the standard DEKF, although a lower number of elements of the covariance matrices needs to be tuned. Indeed, the parameter covariance matrix  $S$  and process noise matrix  $Q^\theta$  pass from 2-by-2 matrices to 1-by-1 matrices, thus requiring two fewer tuning elements. To achieve a proper comparison between the different versions of the DEKF, we tuned the covariance matrices so that the standard DEKF could obtain accurate estimations, and we used the same values for the sleek DEKF, as reported in [Table 1](#).

The proposed SDEKF is tested on the experimental aging dataset from [13] where ten INR21700-M50T battery cells with graphite/silicon anode and nickel manganese cobalt oxides (NMC) cathode are cycled at the constant temperature of 23°C over 10 months to mimic real-world EV operation. While the dynamic discharging current profile is designed to discharge the battery cell through the regulatory urban dynamometer driving schedule (UDDS) from 80% to 20% SOC, the cells are charged through constant current and constant voltage phases. Moreover, to characterize the battery degradation, different reference performance tests (RPTs), i.e., C/20 capacity tests, hybrid pulse power characterization (HPPC), and electrochemical impedance spectroscopy (EIS), are used. The available capacity obtained through the C/20 capacity tests is used to compute the real SOH.

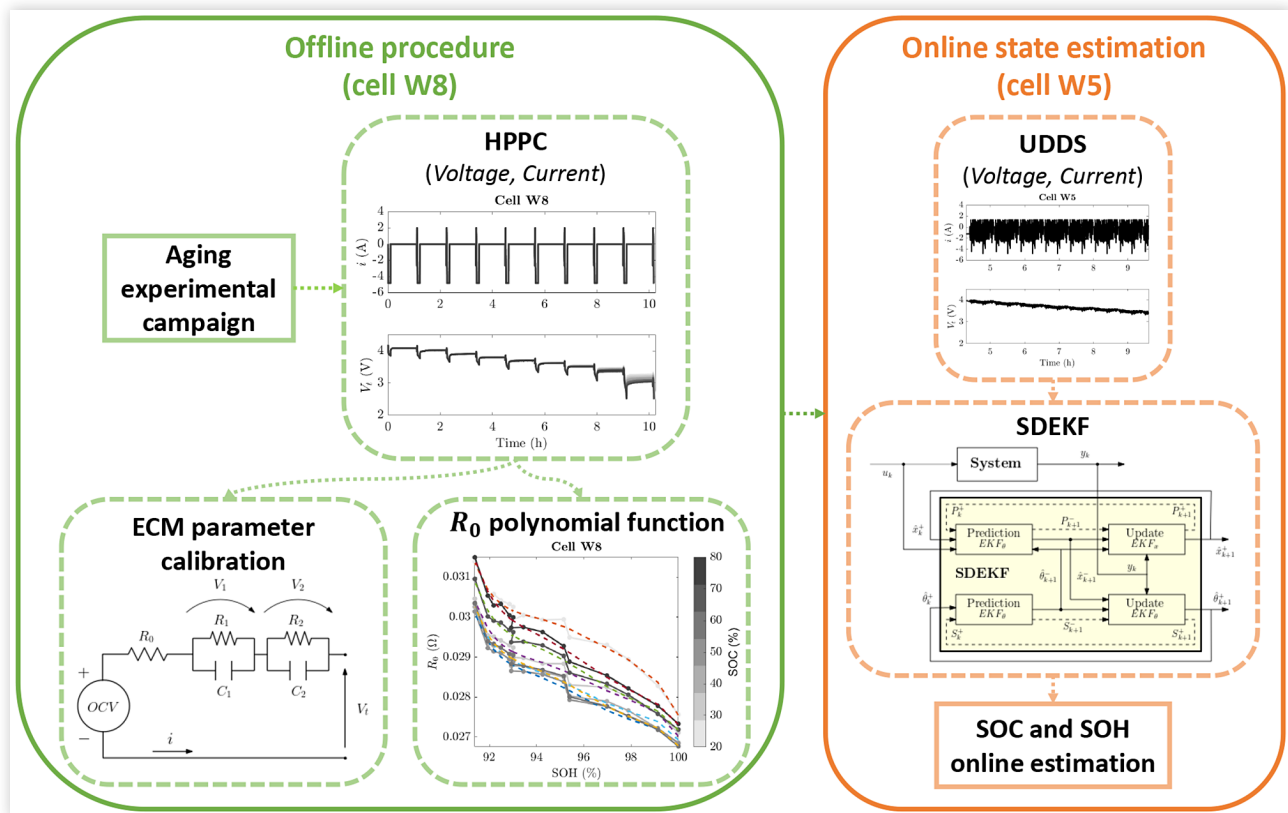
[Fig. 4](#) shows the steps to apply the SDEKF for online SOC and SOH estimation, under the assumption a single

**TABLE 1** Initialization of the filters.

Matrix	Standard DEKF	Sleek DEKF
Initial state covariance $P_0$	$\begin{bmatrix} 10^{-2} & 0 & 0 \\ 0 & 10^{-3} & 0 \\ 0 & 0 & 10^{-3} \end{bmatrix}$	$\begin{bmatrix} 10^{-2} & 0 & 0 \\ 0 & 10^{-3} & 0 \\ 0 & 0 & 10^{-3} \end{bmatrix}$
Initial parameter covariance $S_0$	$\begin{bmatrix} 10^{-2} & 0 \\ 0 & 10^{-4} \end{bmatrix}$	$10^{-2}$
Process noise $Q^x$	$\begin{bmatrix} 10^{-9} & 0 & 0 \\ 0 & 10^{-5} & 0 \\ 0 & 0 & 10^{-5} \end{bmatrix}$	$\begin{bmatrix} 10^{-9} & 0 & 0 \\ 0 & 10^{-5} & 0 \\ 0 & 0 & 10^{-5} \end{bmatrix}$
Process noise $Q^\theta$	$\begin{bmatrix} 10^{-8} & 0 \\ 0 & 10^{-8} \end{bmatrix}$	$10^{-8}$
Measurement noise $R^x$	$10^{-2}$	$10^{-2}$
Measurement noise $R^\theta$	$10^{-2}$	$10^{-2}$

cell (cell W8) is cycled under laboratory conditions through an aging campaign. First, the ECM parameters and the coefficient of the  $R_0$  polynomial function are calibrated using the first HPPC and the different HPPCs over the cell W8 lifetime, respectively. It is worth noting that the

**FIGURE 4** Workflow of the SDEKF estimation algorithm. First, the offline phase is needed to gather the aging dataset, calibrate the ECM parameters and  $R_0$  polynomial function; afterward, the SDEKF is used for online state estimation.



MATLAB function *polyfitn* [19] is used to obtain the polynomial approximation of  $R_0$  as a function of SOC and capacity. Finally, the SDEKF can be used for online estimation on cells different from cell W8. Hence, in this work, the standard DEKF and SDEKF are tested over the 324<sup>th</sup> and 352<sup>th</sup> dynamic UDDS cycles (both corresponding to around 92% SOH) of the W8 and W5 cells, respectively.

Figures 5 and 6 show the estimation results obtained by the DEKF and the proposed SDEKF over cell W8 and cell W5 data, respectively. In the upper subplots, the estimated SOC, capacity, and resistance profiles are compared to the corresponding real values (depicted in black); the lower subplots illustrate the relative estimation errors profiles over the whole experiment. As Figures 5 and 6 show, removing  $R_0$  from the parameters to be estimated by the parameter filter did not cause a significant loss of accuracy by using the polynomial characterization for  $R_0$  in equation (19). Despite the fact that this formulation relies on the estimate of the state of charge and residual capacity, this formulation proved effective enough that the accuracy of the DEKF was not compromised. Considering the SOC error, both DEKFs appear to have a slight tendency towards overestimation. A similar tendency towards overestimation was observed for the capacity, though the difference between the SDEKF and the standard DEKF is negligible (lower than 0.2%). As expected, the difference in the evaluation of  $R_0$  itself is more pronounced. The error obtained by the DEKF does not show a clear tendency towards over or

under-estimation; fluctuations in the value of  $R_0$  are somewhat smoothed out by the filter, as was typically obtained by similar works. The value predicted by the SDEKF has an even smoother trend, as a direct result of its functional formulation, and the prediction error can reach at worst values of up to 9%, compared to 5% for the standard DEKF. Moreover, it is worth noting that both filters obtain accurate estimation also using the W5 cell data, showing the robustness of the algorithms when tested on a cell different from the one used for tuning the ECM parameters.

## Conclusion

In this work, we presented a sleek formulation of the dual extended Kalman filter for state of charge and state of health estimation which does not attempt to estimate the internal resistance  $R_0$  as part of the parameters filter but rather uses a polynomial approximation as a function of SOC and cell capacity.

As a consequence, the sleek EKF requires less tuning effort, which is a critical issue in developing Kalman filter-based state estimators for EV batteries. Despite this, the proposed algorithm does not compromise on prediction accuracy: in particular, it retains virtually equal accuracy with respect to the state of charge and cell capacity, whereas a small but not negligible loss of accuracy was observed for the value of  $R_0$  itself.

**FIGURE 5** State of charge, capacity and ohmic resistance  $R_0$  estimation results and errors obtained for cell W8 by the DEKF and the proposed SDEKF.

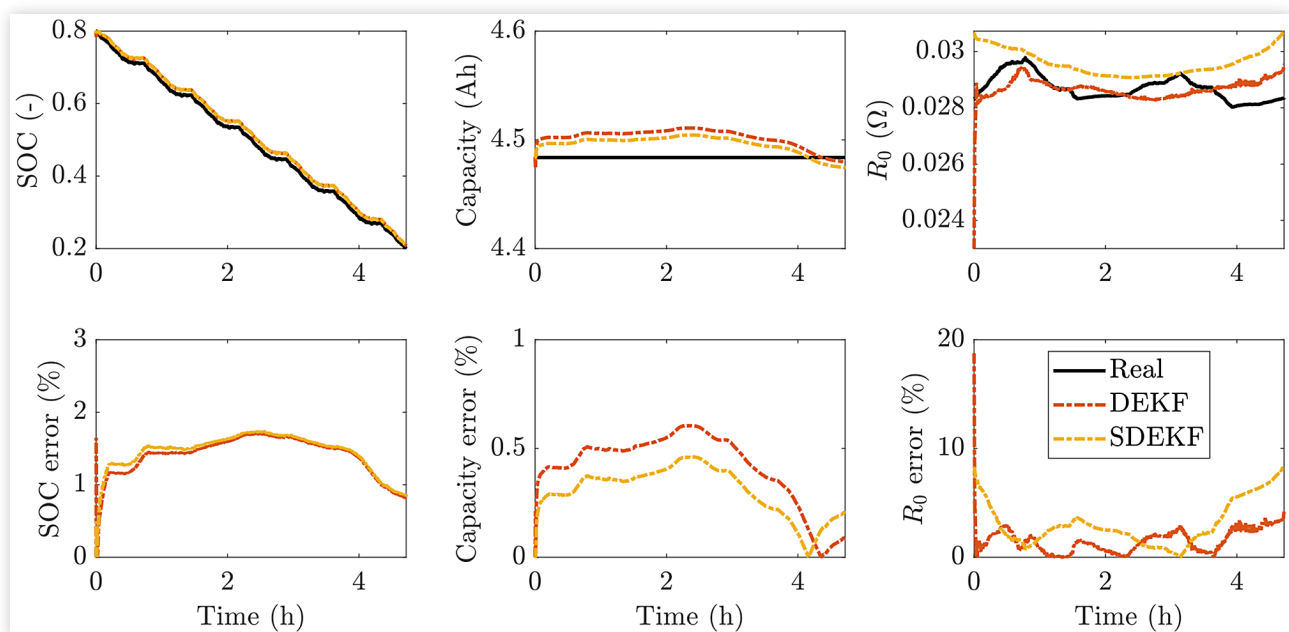
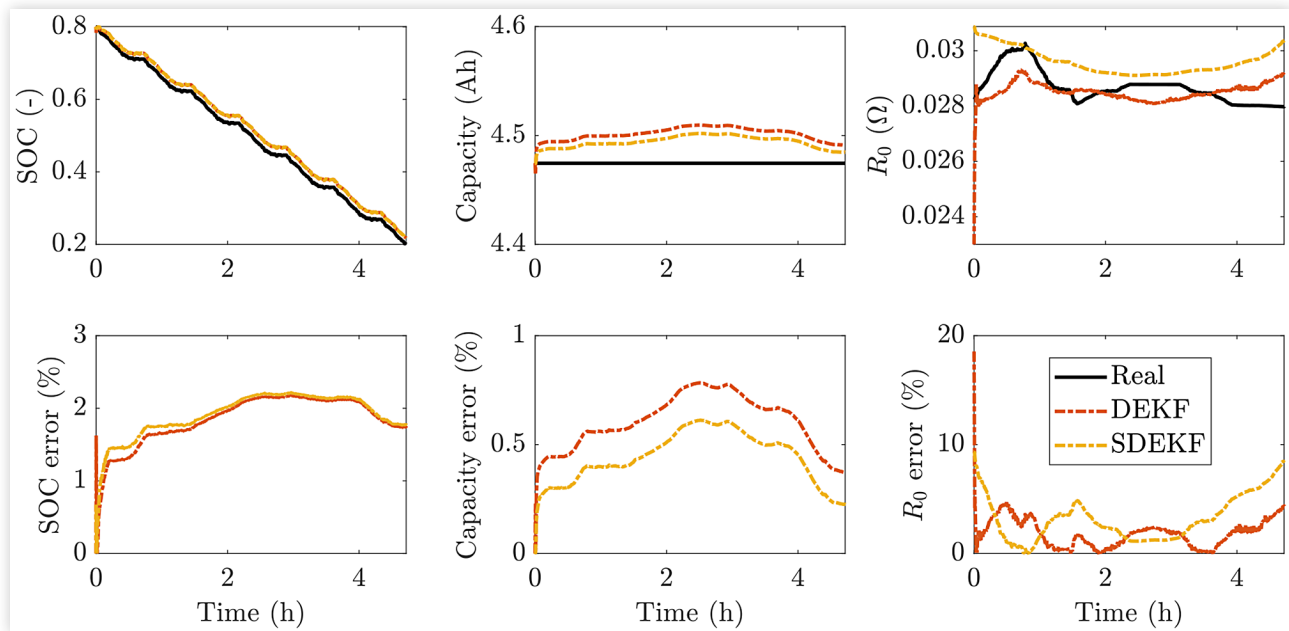


**FIGURE 6** State of charge, capacity and ohmic resistance  $R_0$  estimation results and errors obtained for cell W5 by the DEKF and the proposed SDEKF.



## References

- Plett, G.L., *Battery Management Systems, Volume I: Battery modeling*. Vol. 1 (Artech House, 2015).
- Plett, G.L., "Dual and Joint EKF for Simultaneous SOC and SOH Estimation," in *Proceedings of the 21st Electric Vehicle Symposium (EVS21)*, Monaco, 1-12, 2005.
- Rubagotti, M., Onori, S., and Rizzoni, G., *Automotive Battery Prognostics Using Dual Extended Kalman Filter* (American Society of Mechanical Engineers Digital Collection, Sept. 2010), 257-263.
- Nejad, S., Gladwin, D.T., and Stone, D.A., "On-Chip Implementation of Extended Kalman Filter for Adaptive Battery States Monitoring," in *IECON 2016 - 42nd Annual Conference of the IEEE Industrial Electronics Society*, 5513-5518, October 2016.
- Dai, H., Wei, X., Sun, Z., Wang, J. et al., "Online Cell SOC Estimation of Li-Ion Battery Packs Using a Dual Time-Scale Kalman Filtering for EV Applications," *Applied Energy* 95 (2012): 227-237.
- Li, S., Pischinger, S., He, C., Liang, L. et al., "A Comparative Study of Model-Based Capacity Estimation Algorithms in Dual Estimation Frameworks for Lithium-Ion Batteries under an Accelerated Aging Test," *Applied Energy* 212 (2018): 1522-1536.
- Gao, Y., Nguyen, T., and Onori, S., "Model-Based State-of-Charge Estimation of 28V LiFePO<sub>4</sub> Aircraft Battery," *SAE Int. J. Elec. Veh.* 14, no. 1 (2024), doi:<https://doi.org/10.4271/14-14-01-0003>.
- Azis, N.A., Joelianto, E., and Widyotriatmo, A., "State of Charge (SOC) and State of Health (SOH) Estimation of Lithium-Ion Battery Using Dual Extended Kalman Filter Based on Polynomial Battery Model," in *2019 6th International Conference on Instrumentation, Control, and Automation (ICA)*, July 2019, IEEE.
- Lei, M., Wu, B., Yang, W., Li, P. et al., "Double Extended Kalman Filter Algorithm Based on Weighted Multi-Innovation and Weighted Maximum Correlation Entropy Criterion for Co-Estimation of Battery SOC and Capacity," *ACS Omega* 8 (2023): 15564-15585.
- Wassiliadis, N., Adermann, J., Frericks, A., Pak, M. et al., "Revisiting the Dual Extended Kalman Filter for Battery State-of-Charge and State-of-Health Estimation: A Use-case Life Cycle Analysis," *Journal of Energy Storage* 19 (2018): 73-87.
- Wang, Y., Fang, H., Zhou, L., and Wada, T., "Revisiting the State-of-Charge Estimation for Lithium-Ion Batteries: A Methodical Investigation of the Extended Kalman Filter Approach," *IEEE Control Systems Magazine* 37, no. 4 (2017): 73-96.
- Peñarrocha, I., Pérez, E., Beltran, H., and Díaz-Sanahuja, C., "Dimensionless Tuning Procedure of the Kalman Filter for State-of-Charge Estimators," in *IECON 2023-49th Annual Conference of the IEEE Industrial Electronics Society*, 1-6, 2023, IEEE.
- Pozzato, G., Allam, A., and Onori, S., "Lithium-Ion Battery Aging Dataset Based on Electric Vehicle Realdriving Profiles," *Data in Brief* 41 (2022): 107995.
- Taborelli, C. and Onori, S., "State of Charge Estimation Using Extended Kalman Filters for Battery Management System," in *2014 IEEE International Electric Vehicle Conference (IEVC)*, December 2014, IEEE.
- Plett, G.L., "Extended Kalman Filtering for Battery Management Systems of LIPB-Based HEV Battery



- Packs: Part 1. Background," *Journal of Power sources* 134, no. 2 (2004): 252-261.
16. Guha, A. and Patra, A., "State of Health Estimation of Lithium-Ion Batteries Using Capacity Fade and Internal Resistance Growth Models," *IEEE Transactions on Transportation Electrification* 4 (2018): 135-146.
  17. Saha, B., Goebel, K., Poll, S., and Christophersen, J., "Prognostics Methods for Battery Health Monitoring Using a Bayesian Framework," *IEEE Transactions on Instrumentation and Measurement* 58 (2009): 291-296.
  18. Huang, Y., Li, Y., Jiang, L., Qiao, X. et al., "Research on Fitting Strategy in HPPC Test for Li-Ion Battery," in *2019 IEEE Sustainable Power and Energy Conference (ISPEC)*, 1776-1780, 2019, IEEE.
  19. MATLAB, "Polyfitn," 2016.